Polymer Chemistry

PAPER

View Article Online
View Journal | View Issue

Cite this: *Polym. Chem.*, 2014, **5**, 5330

Amphiphilic block copolymers featuring a reversible hetero Diels-Alder linkage†

Marcel Langer,[ab] Josef Brandt,[c] Albena Lederer,[c] Anja S. Goldmann,[ab] Felix H. Schacher*[d] and Christopher Barner-Kowollik*[ab]

The present article reports the preparation of a novel class of switchable amphiphilic diblock copolymers with a temperature switchable linkage. Reversible addition fragmentation chain transfer (RAFT) polymerization was used to synthesize the individual blocks: for the preparation of the non-polar block, *i.e.* poly(isoprene-*co*-styrene) (P(I-*co*-S)) (9200 g mol^{-1} ≤ M_n ≤ 50 000 g mol^{-1}, 1.22 ≤ $Đ$ ≤ 1.36), a chain transfer agent (CTA, 3-((2-bromo-2-methylpropanoyl)oxy)propyl 2-(((dodecylthio)carbonothioyl) thio)-2-methylpropanoate) carrying a bromine group was employed, ready for subsequent cyclopentadienyl (Cp) transformation. For the preparation of the polar block, triethylene glycol methyl ether acrylate (TEGA) was polymerized (6600 g mol^{-1} ≤ M_n ≤ 35 000 g mol^{-1}, 1.12 ≤ $Đ$ ≤ 1.30) using a RAFT agent carrying a phosphoryl Z-group, which is able to undergo hetero Diels-Alder (HDA) ligation with Cp moieties. Both building blocks were conjugated at ambient temperature in the presence of $ZnCl_2$ as catalyst yielding the amphiphilic block copolymer P(I-*co*-S)-*b*-PTEGA (16 000 g mol^{-1} ≤ M_n ≤ 68 000 g mol^{-1}, 1.15 ≤ $Đ$ ≤ 1.32). To investigate the bonding/debonding capability of the HDA linkage, high temperature nuclear magnetic resonance (HT-NMR) spectroscopy, high temperature dynamic light scattering (HT-DLS) and high temperature size exclusion chromatography (HT-SEC) were carried out, evidencing that efficiently switchable amphiphilic block copolymers were generated (>4 cycles).

Received 7th May 2014
Accepted 2nd June 2014

DOI: 10.1039/c4py00644e

www.rsc.org/polymers

Introduction

Amphiphilic block copolymers are composed of at least one hydrophilic and one hydrophobic block, which are typically covalently bonded. Such macromolecules find many applications, *e.g.* in drug delivery systems,[1,2] membrane filtration and separation systems[3] and electronic materials,[4] based on their ability to phase separate in solution as well as in the solid state. In general, many different architectures can be realized, *e.g.* linear, star shaped or comb like block copolymers.[5] In general, unlike polymer segments are not miscible but the covalent linkage present in block copolymers prevents macroscopic phase separation. Thus, block copolymers undergo microphase separation on the length scale of the constituting building blocks.[6,7] Linear AB diblock copolymers are the simplest block copolymers and have been studied extensively. It was found that depending on the volume fraction of the blocks, the materials form spherical, cylindrical, gyroid, or lamellar nanostructures.[8] Block copolymers with a more complex architecture (*e.g.* ABC triblock terpolymers) can form even more sophisticated nanostructures, including perforated lamellae[9] and helices.[10,11] In light of lithography applications, block copolymers with one block which can be selectively removed are highly interesting.[12] Since 1988,[13] various strategies have developed, *e.g.* degradation *via* UV radiation,[14] chemical etching,[15] or ozonolysis.[16] However, either relatively harsh reaction conditions are required or the method is limited to specific materials. These drawbacks can be avoided by the introduction of an efficiently cleavable junction between adjacent blocks and the use of distinct differences in solubility (in case of amphiphilic block copolymers).[17,18] However, amphiphilic block copolymers featuring a temperature-reversible linkage have not been reported so far.

For the synthesis of block copolymers, two general approaches are possible: either sequential polymerization of several monomers or modular ligation of pre-synthesized

[a]*Soft Matter Synthesis Laboratory, Institut für Biologische Grenzflächen, Karlsruhe Institute of Technology (KIT), Hermann-von-Helmholtz-Platz 1, 76344 Eggenstein-Leopoldshafen, Germany. E-mail: christopher.barner-kowollik@kit.edu*

[b]*Preparative Macromolecular Chemistry, Institut für Technische Chemie und Polymerchemie, Karlsruhe Institute of Technology (KIT), Engesserstr. 18, 76128 Karlsruhe, Germany*

[c]*Leibniz Institut für Polymerforschung, Dresden e.V., Hohe Straße 6, 01069 Dresden, Germany, Technische Universität Dresden, 01062 Dresden, Germany*

[d]*Institut für Organische Chemie und Makromolekulare Chemie and Jena Center for Soft Matter, Friedrich Schiller Universität Jena, 07743 Jena, Germany. E-mail: felix.schacher@uni-jena.de*

† Electronic supplementary information (ESI) available: The experimental part, including the used materials, synthetic procedures and used characterization methods, ^{1}H-, ^{13}C-NMR and ESI-MS spectra of the new RAFT agent, kinetic studies of the polymerization and SEC traces of the polymers before and after Cp-transformation, ^{1}H-NMR spectra of the building blocks and the resulting block copolymer, a table of the calculated ratios from both block copolymers and the content of isoprene and all measured HT-SEC traces. See DOI: 10.1039/c4py00644e

polymeric building blocks can be targeted.[19] Both preparation methods require living polymerization techniques and high end group fidelity, or at least chain growth polymerization techniques featuring living characteristics. Living anionic polymerization is the most powerful technique in terms of polymerization control for the synthesis of polymers with defined molecular weight, architectures and narrow molecular weight distributions.[20] However, substantial restrictions apply to anionic polymerization such as a limited monomer choice associated with the required demanding experimental conditions.[21] In comparison, controlled/living radical polymerization (CLRP) techniques are simpler to implement and have less limitations regarding the monomer choice.[22] *Via* such approaches, good control over molecular weight, architecture, and the molecular weight distribution is obtained. The most common CLRP techniques are nitroxide mediated polymerization (NMP),[23,24] atom transfer radical polymerization (ATRP),[25–27] and reversible addition chain transfer (RAFT)[28,29] polymerization. In order to achieve the successful modular conjugation of polymers, reactions adhering to the strict click criteria[30] are required. Barner-Kowollik and co-workers demonstrated that under certain conditions the hetero Diels-Alder (HDA) reaction between a cyclopentadienyl (Cp) moiety and a C=S double bond of RAFT agents with an electron withdrawing Z group, fulfills these criteria.[31] More recently, the same group demonstrated that the HDA linkage can undergo efficient bonding and debonding behavior *via* a mild temperature gradient.[32]

Herein we present the modular synthesis of amphiphilic diblock copolymers *via* HDA ligation chemistry with the aim of creating reversibly cleavable block junctions. These might be promising candidates for the design of nanostructured materials.[12] As hydrophobic block, a copolymer constituted of styrene and isoprene was chosen as the residual vinyl groups of isoprene in the side chain can be used for subsequent crosslinking. Thus, the mechanical stability and the persistence against solvents of the generated material can be increased. As hydrophilic segment, a polymer with an acrylate backbone is required, since the HDA–RAFT agent is not able to undergo HDA conjugations when a methacrylate monomer is employed in the RAFT polymerization (however, the reverse functions by using a Cp-terminal poly(methacrylate) and a RAFT terminal poly(acrylate)). Moreover, RAFT agents may be sensitive towards amide and amine moieties. Therefore, poly(triethylene glycol methyl ether acrylate) (PTEGA) is employed and both building blocks are combined using HDA chemistry. The reversible HDA linkage enables the cleavage of the resulting amphiphilic block copolymer, potentially also after microphase separation and crosslinking. Thus, this will open up the way to a novel class of nanostructured materials with highly reactive Cp moieties on the surface. We investigate the reversible linkage between both blocks *via* high temperature nuclear magnetic resonance (HT-NMR) spectroscopy, high temperature dynamic light scattering (HT-DLS), and high temperature size exclusion chromatography (HT-SEC).

The experimental data, including the used materials, synthesis procedures and characterization methods, can be found in the ESI.†

Results and discussion

In order to obtain amphiphilic block copolymers with a reversible hetero Diels-Alder (HDA) linkage, the synthetic strategy depicted in Scheme 1 was followed. For the preparation of the polar building block polymer, triethylene glycol methyl ether acrylate (TEGA)[35] was polymerized using a HDA capable RAFT agent.[36] The non-polar building block was synthesized *via* RAFT polymerization with a bromine carrying CTA (DMP-Br). After the polymerization, the bromine end group was substituted with a Cp moiety. Subsequently, both building blocks were ligated *via* a HDA reaction to form the amphiphilic block copolymer P(S-*co*-I)-*b*-PTEGA.

RAFT agent design

The newly developed RAFT agent DMP-Br is based on the well-known CTA DMP.[37,38] It is based on a trithiocarbonate with a tertiary R-group, able to control the polymerizations of styrene and isoprene.[39,40] The facile preparation *via* a Steglich esterification involves 3-hydroxypropyl-2-bromo-2-methylpropanoate[33] to introduce a bromine functionality at the R-group. The bromine substituted R-group can act as an initiator for atom transfer radical polymerizations (ATRP)[34] and can further be substituted with a Cp moiety.[41] Thus, complex block copolymers can be prepared by simultaneous RAFT and ATRP.[42] The molecule was characterized *via* NMR (^{1}H and ^{13}C, see Fig. S1 and S2†) and ESI-MS (see Fig. S3†).

RAFT polymerizations

For the modular block copolymer formation, high end group fidelity of both building blocks is essential. Among the controlled/living radical polymerization techniques, RAFT provides not only high end group fidelity, but concomitantly benefits from higher radical concentrations, compared to nitroxide mediated polymerization (NMP) and atom transfer radical polymerizations (ATRP).[43] Thus, higher polymerization rates and shorter reaction times are accessible. To verify the control afforded by the RAFT process leading to polymers with high end group fidelity, kinetic studies were carried out for the copolymerization of styrene and isoprene using CTA-1 (see Fig. S4, S5 and Table S1†) and the polymerization of TEGA using CTA-2 (see Fig. S6, S7 and Table S2†). The linear increase of the molar mass with good agreement of $M_{n,theo}$ and $M_{n,exp}$ and low $Đ$ values evidences the control of the polymerizations. For each building block (non-polar side with P(S-*co*-I) and polar with PTEGA) two molecular weights have been generated, one lower (P(S-*co*-I): **P1**, M_n = 9200 g mol^{-1}; PTEGA: **P2**, M_n = 6600 g mol^{-1}) and one higher example (P(S-*co*-I): **P4**, M_n = 50 000 g mol^{-1}; PTEGA: **P5**, M_n = 35 000 g mol^{-1}). Due to smaller repeating unit to end group ratio and better solubility features, **P1** and **P2** were subjected to a detailed NMR analysis and DLS experiments, whereas the large differences in solubility of **P4** and **P5** were used for macroscopic separation experiments (will be discussed later).

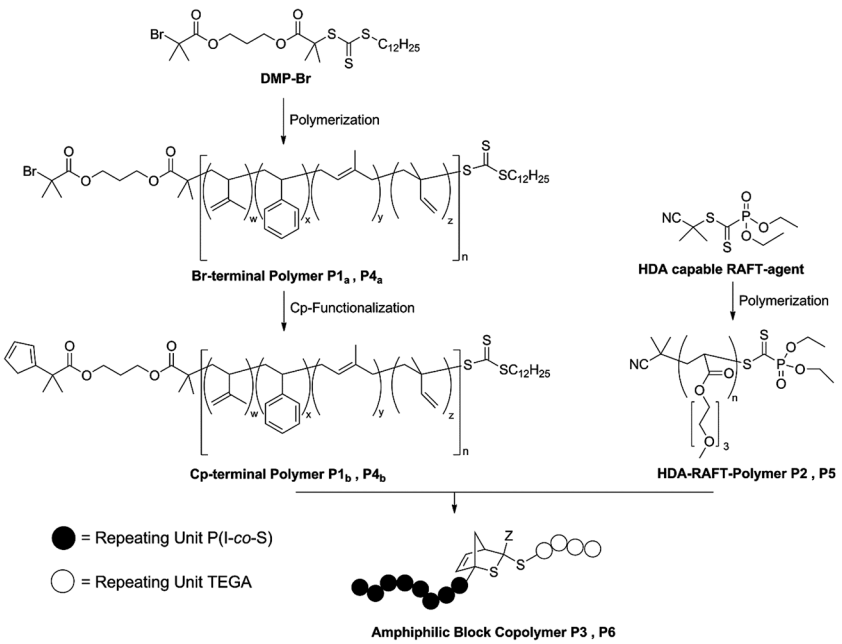

Scheme 1 Synthetic strategy for the preparation of amphiphilic P(S-*co*-I)-*b*-PTEGA block copolymers with a reversible hetero Diels-Alder linkage.

Cp-transformation

In general, two approaches for the substitution of bromine with Cp exist. The use of sodium cyclopentadienyl as source for nucleophilic Cp entails a high reactivity of the Cp-anion towards functional groups such as ester moieties.[44,45] Since two ester moieties are present in the polymer, the NaCp based approach for the Cp transformation is not suitable. Nickelocene ($NiCp_2$) as nucleophilic source, on the other hand, is chosen as a mild and effective transformation that tolerates a wide range of functional groups, including ester moieties.[46] Since it is known that Cp groups undergo dimerization,[47] the comparison of the SEC traces before and after the functionalization of the polymers **P1** and **P4** is essential (see Fig. S8† for polymer **P1** and Fig. S9† for polymer **P4**). The SEC traces of both polymers, **P1** and **P4**, do not show any side products due to dimerization. The successful substitution of bromine with Cp can be verified by the resonances appearing between 6.5 ppm and 6.1 ppm associated with the vinyl protons of the Cp moiety in the ^{1}H-NMR spectra of polymer $\mathbf{P1_b}$ (see Fig. 2). Full conversion – and therefore close to quantitative Cp transformation – was assessed by the successful conjugation of the building blocks $\mathbf{P1_b}$ and **P2** verified *via* SEC.

Block copolymer formation

All conjugation reactions were conducted in ethyl acetate at ambient temperature in the presence of $ZnCl_2$ as catalyst. It is not mandatory to use a catalyst for the polymer conjugation (refer to the *HT-SEC analysis* section). However, more than seven times higher reaction rates are found, especially for larger building blocks. The total concentration of polymers was kept at 50 mg mL^{-1} for the preparation of **P3** and **P6**. The SEC traces for the generated block copolymers and the corresponding building blocks are presented in Fig. 1.

As expected, the resulting block copolymer **P3** shows a significant shift to lower retention volume, compared to the building blocks $\mathbf{P1_b}$ and **P2**. Moreover, the $Đ$ value of **P3** ($Đ = 1.15$) is in between the values of the building blocks $\mathbf{P1_b}$ and **P2** ($\mathbf{P1_b}$: $Đ = 1.22$ and **P2**: $Đ = 1.12$). The low $Đ$ value and the shift to a lower retention volume indicate the successful conjugation and thus, close to quantitative Cp-transformation of the building block **P1**.[48,49] For the block copolymer with higher molecular weight (**P6**), the shift to lower retention volumes, compared to its building blocks $\mathbf{P4_b}$ and **P5**, is less pronounced than for polymer **P3**. This observation is associated with the fact that high molecular weight polymers have a small retention volume and therefore have a larger effect on the resulting molecular weight shift after ligation compared to polymers with lower molecular weights. Thus, the shift of the block copolymer compared to its building blocks is in the expected range. Furthermore, the $Đ$ value of **P6** ($Đ = 1.32$) is in between the values of the building blocks $\mathbf{P4_b}$ and **P5** ($\mathbf{P4_b}$: $Đ = 1.36$ and **P5**: $Đ = 1.30$). Again, low $Đ$ values and the shift to lower retention volumes indicate a successful and quantitative conjugation. In addition, **P1**, **P2** and **P3** were analyzed *via* ^{1}H-NMR spectroscopy (see Fig. S10†). The spectrum of the block copolymer **P3** is the sum of the resonances from the individual building block polymers $\mathbf{P1_b}$ and **P2**. The molar ratio of PTEGA and P(S-*co*-I) in the resulting block copolymer can be determined by comparison of the integrals from the resonances of the individual building blocks. A table of the calculated ratios from both block copolymers and the content of isoprene is shown in the ESI (see Table S3†). Inspection of the ^{1}H-NMR spectra of the polymers $\mathbf{P1_b}$ and **P3** in the region of the vinyl moiety (6.7 ppm–5.2 ppm,

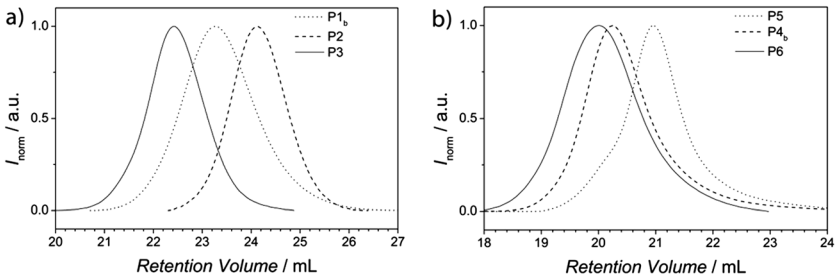

Fig. 1 (a) SEC traces of the polar building block PTEGA (**P2**, dashed line, $M_n = 6600$ g mol^{-1} (PMMA calibration), $Đ = 1.12$), the non-polar building block P(S-*co*-I) (**P1$_b$**, dotted line, $M_n = 9200$ g mol^{-1} (PS calibration), $Đ = 1.22$) and the resulting block copolymer P(S-*co*-I)-*b*-PTEGA (**P3**, solid line, $M_n = 16\,000$ g mol^{-1} (PS calibration), $Đ = 1.15$). (b) SEC traces of the polar building block PTEGA (**P5**, dotted line, $M_n = 35\,000$ g mol^{-1} (PMMA calibration), $Đ = 1.30$), the unpolar building block P(S-*co*-I) (**P4$_b$**, dashed line, $M_n = 50\,000$ g mol^{-1} (PS calibration), $Đ = 1.36$) and the resulting block copolymer P(S-*co*-I)-*b*-PTEGA (**P6**, solid line, $M_n = 68\,000$ g mol^{-1} (PS calibration), $Đ = 1.32$).

see Fig. 2) clearly indicates the strong decrease of the resonances of the Cp moiety from polymer **P1$_b$** after the HDA reaction. Consequently, the block copolymer **P3** reveals a new resonance, corresponding to a proton of the HDA reaction product. The two resonances at 6.16 ppm and 5.72 ppm of the Cp moiety and the HDA reaction product are essential for following the bonding and debonding of the hetero Diels-Alder linkage by HT-NMR analysis.

HT-NMR analysis

A (H)DA reaction is at all times in an equilibrium with its retro (H)DA reaction. At ambient temperature, the equilibrium of the HDA reaction of **P1$_b$** with **P2** is completely shifted towards the HDA reaction product, *i.e.* the block copolymer **P3**. However, by increasing the temperature the retro HDA reaction is favored and the equilibrium shifts towards the reactants **P1$_b$** and **P2**. HT-NMR analysis allows for the determination of the temperature when the equilibrium is completely shifted towards the reactants **P1$_b$** and **P2**. Thus, ^{1}H-NMR spectra of the block copolymer **P3** were recorded while increasing the temperature from 25 °C to 85 °C (see Fig. 3). To obtain information of the position of the equilibrium between the block copolymer **P3** and the reactants **P1$_b$** and **P2**, the region of the resonance of the Cp proton H_a (6.2–6.0 ppm) and the region from the resonance of the proton from the HDA reaction product H_b (5.85–5.6 ppm) were inspected. To ensure equilibrium conditions for each

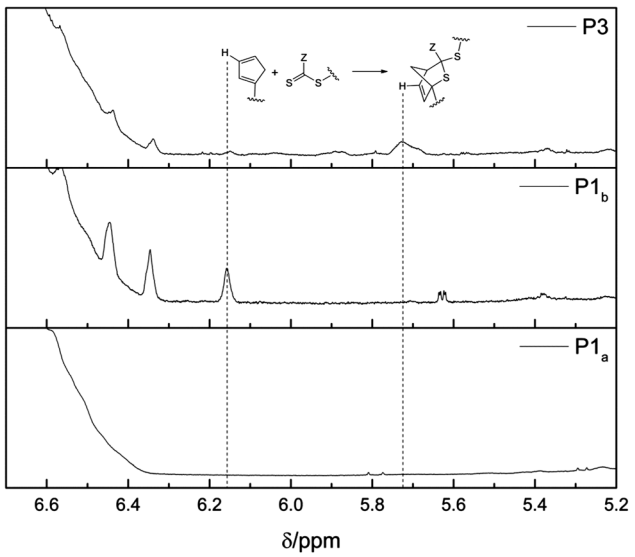

Fig. 2 ^{1}H-NMR spectra of the relevant region (500 MHz, $CDCl_3$, ambient temperature) of polymer **P1** before (**P1$_a$**) the Cp-transformation, after (**P1$_b$**) the Cp-transformation and of the block copolymer **P3**. Comparing the spectra of **P1$_a$** and **P1$_b$**, the resonance of the cyclopentadienyl moiety can be identified (left dashed line). After the block copolymer formation, the Cp-associated resonance disappears and an additional resonance associated with the DA reaction product in a different region is visible (**P3**, right dashed line). An enlargement of the relevant peaks employed for HT-NMR (recorded in toluene-d_6/DMSO-d_6) is depicted for the 25 °C sample in Fig. 3.

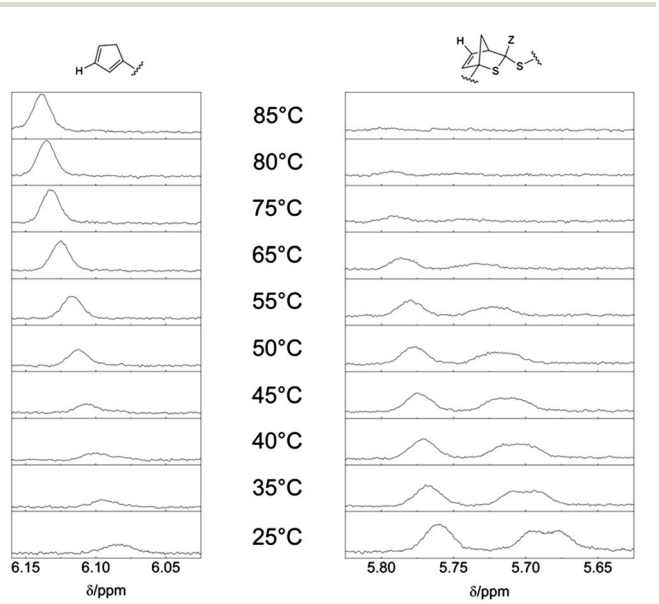

Fig. 3 ^{1}H-NMR spectra (400 MHz, toluene-d_8–DMSO-d_6, 1 : 1) of the block copolymer **P3** at variable temperatures. The resonances of the Cp moiety are depicted on the left hand side (6.2–6.0 ppm, H_a) and the resonances associated with the DA reaction product are depicted on the right hand side (5.85–5.6 ppm, H_b). As the temperature increases, the intensity of the Cp resonance (left side) increases, whereas the intensity of the DA reaction product resonance decreases (right side). Above 85 °C the building blocks are completely separated.

temperature step, successive NMR spectra have been recorded until the actual spectrum is identical with the one recorded before. From 45 °C to 85 °C, the intensity of the resonance of the Cp moiety is increasing continuously. Simultaneously, the intensity of the resonance of the HDA reaction product is decreasing. At 85 °C, the resonance of the proton of the hetero Diels-Alder product completely disappears, indicating complete debonding. The complete disappearance of the peaks at 5.85–5.6 ppm and concurrent appearance of the resonance peak at 6.2–6.0 ppm indicate that the equilibrium is completely shifted towards the building blocks **P1$_b$** and **P2**. The shift of the signals towards a lower field is due to the increasing temperature. The NMR experiment was performed in a mixture of toluene-d_8 and DMSO-d_6 (1 : 1). The solvent mixture was used to ensure a moderate polarity to keep both building blocks in solution after debonding. In addition, a high boiling point was preferred because the cleavage temperature is relatively high. Having determined the cleavage temperature, further HT-NMR experiments have been performed in $CDCl_3$ in an NMR pressure tube in the presence of $ZnCl_2$ as catalyst. Note that the different employed NMR solvents slightly affect the resonances appearance and position.

To evidence that the bonding and debonding of the building blocks **P1$_b$** and **P2** is reversible with temperature, NMR spectra of the block copolymer **P3** were conducted and cycled 4 times between 25 °C and 90 °C (see Fig. 4). Again, the regions of the resonance from the Cp proton (6.1–6.0 ppm) and of the proton of the HDA reaction product (5.85–5.6 ppm) were investigated.

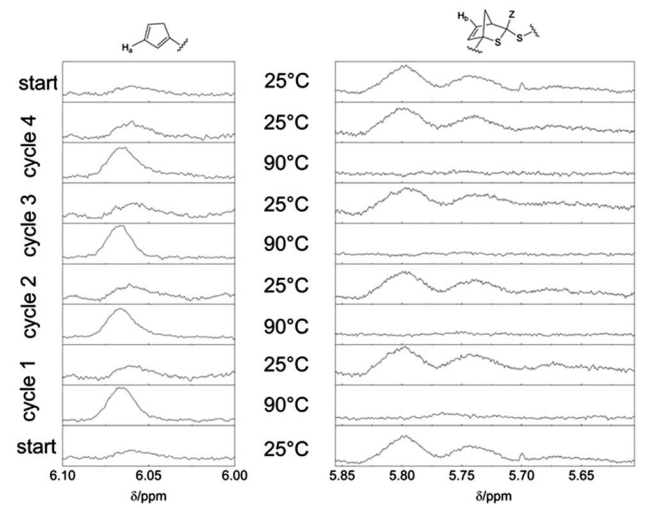

Fig. 4 ^{1}H-NMR spectra (400 MHz, $CDCl_3$) of the block copolymer **P3** at alternating temperatures in four heating/cooling cycles between 25 °C and 90 °C. The resonances of the cyclopentadienyl moiety are depicted on the left side (6.1–6.0 ppm, H_a) and the resonances associated with the DA reaction product are shown on the right side (5.85–5.6 ppm, H_b). After the cleavage at 90 °C, the block copolymer **P3** is reformed at 25 °C. For better comparison, the starting spectrum is depicted at the bottom and on top of the figure. Note that the forward ligation is not 100% quantitative, due to the Diels-Alder reaction being an equilibrium reaction and some limited debonded material remains at ambient temperature.

The bonding/debonding behavior can be observed over all 4 cycling processes. For every cycle, the resonance of the Cp moiety has full intensity at 90 °C, whereas in the region of the HDA reaction product only the baseline can be detected, revealing complete transformation into the two separate building blocks. Concomitantly, the resonance of the Cp moiety disappears for each cycle at 25 °C with highest intensity of the resonance of the HDA reaction product H_b. For the cleavage of the block copolymer at 90 °C an equilibrium time of approximately 30 min was observed. Complete rebonding was achieved after 24 h at 25 °C. The difference in reaction time, compared to the synthesis of **P3** (16 h), can be explained by the absence of stirring of the polymer solution in the NMR tube and thus the bonding is only diffusion controlled, leading to longer reaction time for the block copolymer formation. In $CDCl_3$ no shift of the signals towards a lower field at elevated temperatures could be observed.

HT-DLS analysis

To further underpin the results of the HT-NMR experiments, HT-DLS analysis of the block copolymer **P3** has been carried out. Since no pressure stable DLS cuvettes were available, the choice of solvents was limited by their boiling points and scattering properties as well as their ability to dissolve both individual building blocks. **P3** was dissolved in a mixture of *N*,*N*-dimethylacetamide (DMAc, 80 vol%) and toluene (20 vol%) in the presence of $ZnCl_2$ as catalyst revealing the best possible conditions for the HT-DLS measurements. Representative examples of autocorrelation functions and the resulting size distributions can be found in Fig. S11 and S12,† respectively. For the block copolymer, unimers with a radius of close to 2.5 nm are detected at 30 °C (refer to Fig. 5). When the sample is heated to 90 °C, the detected radius decreases to values below 2.0 nm, hinting at the block copolymer being cleaved into the individual building blocks, which form significantly smaller unimers. As soon as the temperature is decreased again to 30

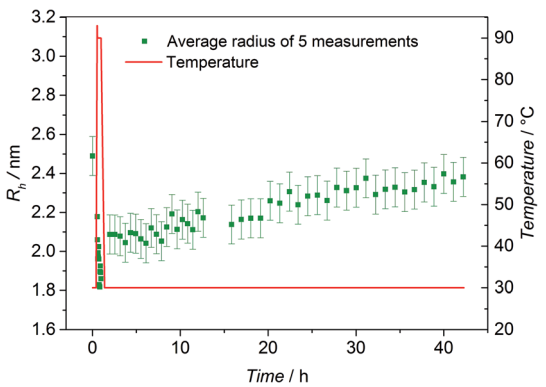

Fig. 5 HT-DLS experiment of block copolymer **P3** in DMAc in the presence of $ZnCl_2$ as catalyst. The green squares depict the average radius of 5 subsequently measured values in the specified time interval. The experimental standard deviation is close to 0.1 nm. Due to the fast and large change of the actual radius when the sample is heated at 90 °C, no average radius is calculated for that temperature. The red solid line displays the temperature evolution.

°C, the block copolymer – and hence the corresponding unimers – start to reform and the radius increases again continuously with time up to the initially recorded average size (2.4 nm).

To examine the reversible bonding and debonding behavior of the HDA linkage, 4 temperature cycles between 30 °C and 90 °C were performed (refer to Fig. 6). At 90 °C, the system was allowed to equilibrate for 30 min until no further changes in R_h could be detected. Similarly, at 30 °C, the detected radius was measured after the equilibrium was established. For every temperature switch the expected change of the detected radius can be observed.

In contrast, the building block (**P1$_b$**) as reference exhibits a radius of approximately 1.6 nm and no significant change with varying temperature could be observed. However, the respective radii for each cycle at 90 °C and at 30 °C vary more than expected (90 °C: 1.5–1.7 nm; 30 °C: 1.9–2.3 nm). A possible explanation is associated with the change of the actual ratio of the employed solvent mixture during the measurement. Since sealed cuvettes are not commercially available and thus could not be used, a certain amount of solvent evaporates constantly during the experiment (boiling point DMAc: 165 °C, boiling point toluene: 110 °C). Thus, continually solvent had to be added, possibly affecting the experiment and the data evaluation. The solubility of the polymers is influenced by the composition of the solvent mixture. A change in the ratio of toluene to DMAc can possibly lead to small aggregates that affect the measured R_h averages. In addition, the data evaluation depends on the solvent composition since the calculated R_h is indirectly proportional to the solution viscosity. In summary, the results of the HT-DLS experiments clearly underpin the results of the HT-NMR analysis.

HT-SEC analysis

To further support the results of the HT-NMR and HT-DLS analysis, cycled HT-SEC experiments were performed. A solution of the block copolymer **P3** in TCB was prepared (5 mg mL^{-1}) and placed into the autosampler (set to 90 °C). The sample was measured immediately in order to monitor the bonded state (see Fig. 7, solid black line, 0 min). However, it must be noted that at this point 100% bonding cannot be monitored because the sample is subjected to 90 °C for approximately 7–10 minutes during the analysis and, therefore, debonding of the hetero Diels-Alder linkage partially takes place before the differential refractive index (dRI) detector is reached. Thus, three distinct distributions can be observed, *i.e.* the two building blocks and the block copolymer. The unpolar building block shows a positive dRI signal at a retention time of close to 7.8 min (peak maximum), whereas the polar block shows a large negative dRI signal at approximately 8.6 min retention time (peak maximum). The block copolymer reveals a small negative signal at a retention time of close to 8.1 min. The calculated distributions are depicted as dashed lines. The assignments are based on SEC measurements of the particular building blocks. For validation, the sum of the three calculated distributions is compared with the experimental data, showing good agreement.

Next, the sample was allowed to equilibrate for 30 minutes at 90 °C where the retro HDA reaction proceeds completely. Subsequently, a new chromatogram was recorded, representing the debonded state (refer to Fig. 8, black solid line, 30 min) with maximum intensity (respectively in positive and negative direction) of the building blocks. Again, the calculated distributions are depicted in dashed lines. The distribution of the block copolymer disappears completely.

Next, the sample was removed from the autosampler and kept at ambient temperature for 5 days in which the HDA conjugation of the building blocks takes place (without the presence of any catalyst). This procedure was repeated 4 times, all SEC traces can be found in Fig. S13.† The signal intensities have been evaluated in detail by deconvolution of the chromatograms to determine the peak areas. The results are displayed in the inset diagram in Fig. 8. The trend of the data clearly demonstrates the expected effects: the peak area and

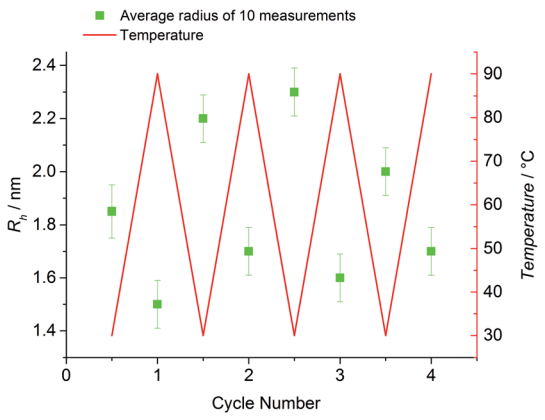

Fig. 6 HT-DLS cycles of block copolymer **P3** in DMAc (80 vol%) and toluene (20 vol%) in the presence of $ZnCl_2$ as catalyst. The green squares represent the average radius of 10 subsequently measured values with an experimental standard deviation of 0.1 nm. The red solid line displays the temperature evolution.

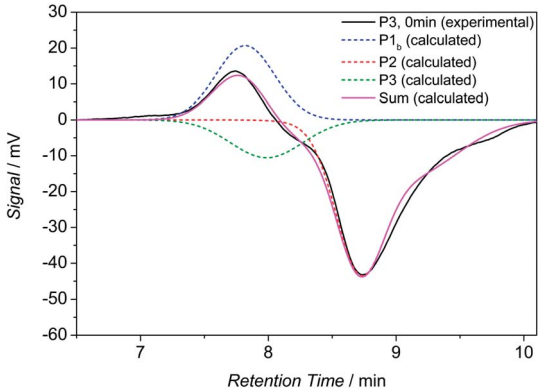

Fig. 7 SEC trace of **P3** in TCB at 90 °C. The black solid line represents the measurement immediately after the sample was placed into the autosampler (0 min), the dashed lines indicate the mathematically fitted fractions of the polar block (**P2**), the non-polar block (**P1$_b$**) and the block copolymer (**P3**). The pink solid line represents the sum of all theoretical peaks.

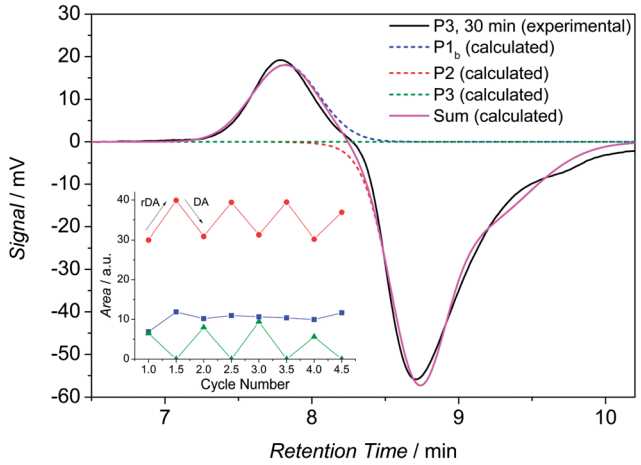

Fig. 8 SEC trace of **P3** in TCB at 90 °C. The black solid line represents the measurement 30 min after the sample was placed into the autosampler, the dashed lines indicate the mathematically fitted fractions of the polar block (**P2**), the non-polar block (**P1$_b$**) and the block copolymer (**P3**). The pink solid line represents the sum of all theoretical peaks. The inset diagram shows the evolution of the peak areas of the three distributions, alternating for every bonding/debonding cycle.

thus the concentration of both building blocks increases during the retro DA reaction and it decreases during the DA reaction. As expected, the observation for the block copolymer is inversed (the intensity of **P1$_b$** is minor because of the low d*n*/d*c* value and thus the changes in peak area are less pronounced). The separation of the specific polymers on the SEC column is not purely entropically driven but also due to enthalpic interactions (adsorption of polar polymers on the column material at high temperatures with TCB as eluent was already observed in other experiments). Thus, the retention time of the amphiphilic block copolymer is in between the retention times of the constituting building blocks. A standard calibration for calculating molar masses is not feasible since enthalpic interactions are occurring. However, the constant difference of the RI signal intensities of the building blocks between the measurements after 0 min and 30 min for the respective cycles confirms again the temperature dependent cleavage of the HDA linkage, here without the presence of any catalyst.

Macroscopic cleavage

To corroborate the results of the aforementioned bonding and debonding studies of the amphiphilic block copolymer, the thermo-responsiveness and the opposite polarities of the building blocks have been harnessed for a macroscopic separation study. First, an aqueous dispersion of the block copolymer **P6** was generated. Therefore, **P6** was dissolved in THF and subsequently added to water. Next, the THF was removed under reduced pressure. The dispersion was heated at 90 °C for 30 min and then cooled to ambient temperature (see Fig. 9). At 90 °C the amphiphilic block copolymer **P6** is debonded to yield the building blocks **P4$_b$*** and **P5***. **P4$_b$*** is not soluble in water and

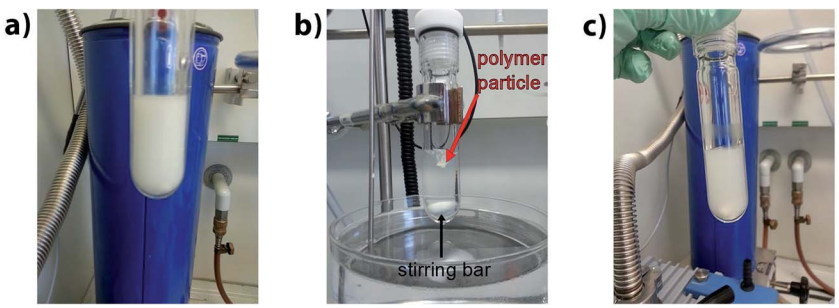

Fig. 9 Images of the macroscopic cleavage of the block copolymer **P6**, into the building block polymers **P4$_b$*** and **P5***. (a) Block copolymer dispersion in water at ambient temperature. (b) At 90 °C the building blocks are separated. Due to the LCST of **P5**, the building block polymers **P4$_b$*** and **P5*** aggregate and form a macroscopic agglomerate (red arrow). (c) Cooled to ambient temperature, **P5*** dissolves in water, whereas **P4$_b$*** forms an aqueous dispersion.

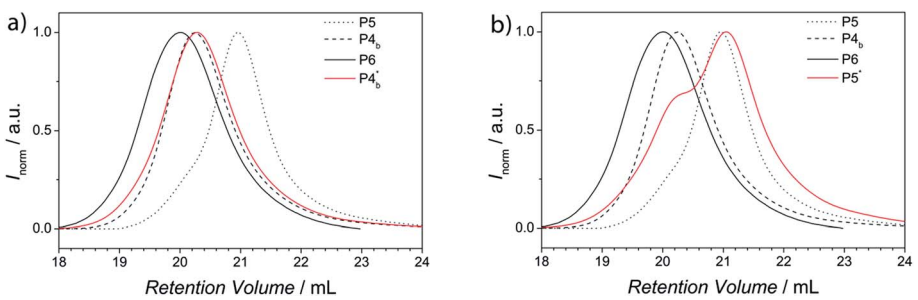

Fig. 10 SEC traces of the building blocks after macroscopic separation (a) non-polar block P(S-*co*-I), **P4$_b$***, solid red line; (b) polar block PTEGA, **P5***, solid red line), in comparison to the initial building blocks (**P4$_b$** and **P5**) and the block copolymer (**P6**).

thus remains as precipitate. In contrast, **P5*** is soluble in water, yet has a lower critical solution temperature (LCST) at 70 °C. Above the LCST, **P5** does not precipitate as a solid, but as a sticky liquid. Hence, at 90 °C the polymers **P4$_b$*** and **P5*** aggregate and form a large macroscopic agglomerate. When the mixture is cooled to ambient temperature **P5*** dissolves in water, whereas **P4$_b$*** remains insoluble and forms an aqueous dispersion. Finally, **P4$_b$*** and **P5*** (one dissolved in water, the other as dispersion) have been separated *via* centrifugation (for a separation *via* filtration, the particles of the dispersion have been too small in size).

The obtained polymers **P4$_b$*** and **P5*** were analyzed *via* SEC and compared with the SEC traces of the original building blocks **P4$_b$** and **P5** and the block copolymer (see Fig. 10). For **P4$_b$*** the SEC trace is in good agreement with the SEC trace of **P4$_b$**. However, the SEC trace of **P5*** shows a shoulder in the retention volume region of **P4$_b$**. A small amount of **P4$_b$*** particles were probably not fully separated from the solution of **P5***. These findings again support the temperature-dependent studies *via* HT-NMR and HT-DLS discussed earlier.

Conclusions

An in-depth study on a novel amphiphilic bonding/debonding on demand system, *i.e.* the amphiphilic block copolymer P(S-*co*-I)-*b*-PTEGA featuring a temperature switchable linkage, is presented. Reversible addition fragmentation chain transfer (RAFT) polymerization was used to synthesize the constituting building blocks. Therefore, a novel trithiocarbonate RAFT agent was synthesized carrying a bromine moiety at the tertiary R-group for subsequent Cp transformation of the end group to afford P(S-*co*-I). Subsequently, a HDA capable, phosphorous RAFT agent was used for the controlled polymerization of triethylene glycol methyl ether acrylate. The building blocks were ligated by a hetero Diels-Alder reaction at ambient temperature in the presence of $ZnCl_2$ as catalyst to prepare the amphiphilic block copolymer. The bonding/debonding capability of P(S-*co*-I)-*b*-PTEGA was evidenced by high temperature nuclear magnetic resonance (HT-NMR) spectroscopy, high temperature dynamic light scattering (HT-DLS) and high temperature size exclusion chromatography (HT-SEC). The current study shows that the concept of reversible HDA linkages in block copolymers can be expanded to amphiphilic systems. The linkage can be repeatedly temperature cycled with high molecular precision, thus paving the way for the use of the herein introduced synthetic platform technology for the preparation of nanostructured and, perspectively, porous materials.

Abbreviations

AIBN	2,2′-Azobis(2-methylpropionitrile)
ATRP	Atom transfer radical polymerization
CLRP	Controlled/living radical polymerization
Cp	Cyclopentadienyl
CTA	Chain transfer agent
DCC	*N*,*N*′-dicyclohexylcarbodiimide
DCM	Dichloromethane
DMAc	Dimethylacetamide
DMAP	4-(Dimethylamino)pyridine
DMP-Br	3-((2-Bromo-2-methylpropanoyl)oxy)propyl 2-(((dodecylthio)carbonothioyl)thio)-2-methylpropanoate
DMSO	Dimethylsulfoxide
dRI	Differential refractive index
ESI-MS	Electrospray ionization-mass spectrometry
HDA	Hetero Diels-Alder
HT-DLS	High temperature dynamic light scattering
HT-NMR	High temperature nuclear magnetic resonance
HT-SEC	High temperature size exclusion chromatography
LCST	Lower critical solution temperature
MHS	Mark–Houwink–Sakurada
NMP	Nitroxide mediated polymerization
PI	Polyisoprene
PMMA	Polymethylmethacrylate
PS	Polystyrene
PTEGA	Polytriethyleneglycol methylether acrylate
RAFT	Reversible addition–fragmentation chain transfer
TCB	1,2,4-Trichlorobenzene
THF	Tetrahydrofuran
VAm-110	2,2′-Azobis(*N*-butyl-2-methylpropionamide)

Acknowledgements

F. H. S. and C. B.-K. acknowledge funding from the German ministry for education and research (BMBF) in the framework of the Biotechnology 2020+ initiative (031A119A and 031A119B). C. B.-K. acknowledges continued support from the Karlsruhe Institute of Technology (KIT) in the context of the Helmholtz BIF program supporting the Soft Matter Synthesis (SML) platform. Dr Leonie Barner is thanked for managing the SML platform. In addition, F. H. S. is grateful to the Verband der Chemischen Industrie (VCI) for a fellowship. The authors thank Christian Pietsch and Christoph Hörenz for helpful discussions.

References

1 M. L. Adams, A. Lavasanifar and G. S. Kwon, *J. Pharm. Sci.*, 2003, **92**, 1343–1355.
2 G. Gaucher, M.-H. Dufresne, V. P. Sant, N. Kang, D. Maysinger and J.-C. Leroux, *J. Controlled Release*, 2005, **109**, 169–188.
3 F. H. Schacher, P. A. Rupar and I. Manners, *Angew. Chem., Int. Ed.*, 2012, **51**, 7898–7921.
4 H.-C. Kim, S.-M. Park and W. D. Hinsberg, *Chem. Rev.*, 2010, **110**, 146–177.
5 A. W. York, S. E. Kirkland and C. L. McCormick, *Adv. Drug Delivery Rev.*, 2008, **60**, 1018–1036.
6 F. S. Bates and G. H. Fredrickson, *Annu. Rev. Phys. Chem.*, 1990, **41**, 525–557.
7 K. Koo, H. Ahn, S.-W. Kim, D. Y. Ryu and T. P. Russell, *Soft Matter*, 2013, **9**, 9059–9071.

8 N. A. Lynda, A. J. Meulerb and M. A. Hillmyer, *Prog. Polym. Sci.*, 2008, **33**, 875–893.
9 F. H. Schacher, H. Sugimori, H. Song, H. Jinnai and A. H. E. Müller, *Macromolecules*, 2012, **45**, 7956–7963.
10 H. Jinnai, T. Kaneko, K. Matsunaga, C. Abetz and V. Abetz, *Soft Matter*, 2009, **5**, 2042–2046.
11 F. H. Schacher, T. Rudolph, M. Drechsler and A. H. E. Müller, *Nanoscale*, 2011, **3**, 288–297.
12 C. J. Hawker and T. P. Russell, *MRS Bull.*, 2005, **30**, 952–966.
13 J. S. Lee, A. Hirao and S. Nakahama, *Macromolecules*, 1988, **21**, 274–276.
14 J. Bang, S. H. Kim, E. Drockenmuller, M. J. Misner, T. P. Russell and C. J. Hawker, *J. Am. Chem. Soc.*, 2006, **128**, 7622–7629.
15 J. M. Leiston-Belanger, T. P. Russell, E. Drockenmuller and C. J. Hawker, *Macromolecules*, 2005, **38**, 7676–7683.
16 P. Mansky, C. K. Harrison, P. M. Chaikin, R. A. Register and N. Yao, *Appl. Phys. Lett.*, 1996, **68**, 2586–2588.
17 J. T. Goldbach, T. P. Russell and J. Penelle, *Macromolecules*, 2002, **35**, 4271–4276.
18 H. Zhao, W. Gu, E. Sterner, T. P. Russell, E. B. Coughlin and P. Theato, *Macromolecules*, 2011, **44**, 6433–6440.
19 N. Hadjichristidis, M. Pitsikalis and H. Iatrou, *Adv. Polym. Sci.*, 2005, **189**, 1–124.
20 K. Hong, D. Uhrig and J. W. Mays, *Curr. Opin. Solid State Mater. Sci.*, 1999, **4**, 531–538.
21 N. Hadjichristidis, H. Iatrou, S. Pispas and M. Pitsikalis, *J. Polym. Sci., Part A: Polym. Chem.*, 2000, **38**, 3211–3234.
22 W. A. Braunecker and K. Matyjaszewski, *Prog. Polym. Sci.*, 2007, **32**, 93–146.
23 G. Moad and E. Rizzardo, *Macromolecules*, 1995, **28**, 8722–8728.
24 D. A. Shipp, *Polym. Rev.*, 2011, **51**, 99–103.
25 M. Kato, M. Kamigaito, M. Sawamoto and T. Higashimura, *Macromolecules*, 1995, **28**, 1721–1723.
26 J.-S. Wang and K. Matyjaszewski, *J. Am. Chem. Soc.*, 1995, **117**, 5614–5615.
27 K. Matyjaszewski, *Macromolecules*, 2012, **45**, 4015–4039.
28 J. Chiefari, Y. K. Chong, F. Ercole, J. Krstina, J. Jeffery, T. P. T. Le, R. T. A. Mayadunne, G. F. Meijs, C. L. Moad, G. Moad, E. Rizzardo and S. H. Thang, *Macromolecules*, 1998, **31**, 5559–5562.
29 *Handbook of RAFT Polymerization*, ed. C. Barner-Kowollik, Wiley-VCH, Weinheim, Germany, 2008.
30 (*a*) H. C. Kolb, M. G. Finn and K. B. Sharpless, *Angew. Chem., Int. Ed.*, 2001, **40**, 2004–2021; (*b*) C. Barner-Kowollik, F. E. Du Prez, P. Espeel, C. J. Hawker, T. Junkers, H. Schlaad and W. Van Camp, *Angew. Chem., Int. Ed.*, 2011, **50**, 60–62.
31 M. Glassner, G. Delaittre, M. Kaupp, J. P. Blinco and C. Barner-Kowollik, *J. Am. Chem. Soc.*, 2012, **134**, 7274–7277.
32 N. K. Guimard, J. Ho, J. Brandt, C. Y. Lin, M. Namazian, J. O. Mueller, K. K. Oehlenschlager, S. Hilf, A. Lederer, F. G. Schmidt, M. Coote and C. Barner-Kowollik, *Chem. Sci.*, 2013, **4**, 2752–2759.
33 C. N. Urbani, A. B. Craig, M. R. Whittaker and M. J. Monteiro, *Macromolecules*, 2008, **41**, 1057–1060.
34 J. T. Lai, D. Filla and R. Shea, *Macromolecules*, 2002, **35**, 6754–6756.
35 F. Hua, X. Jiang, D. Li and B. Zhao, *J. Polym. Sci., Part A: Polym. Chem.*, 2006, **44**, 2454–2467.
36 A. Alberti, M. Benaglia, M. Laus and K. Sparnacci, *J. Org. Chem.*, 2002, **67**, 7911–7914.
37 X. Yin, A. S. Hoffman and P. S. Stayton, *Biomacromolecules*, 2006, **7**, 1381–1385.
38 C. W. Scales, A. J. Convertine and C. L. McCormick, *Biomacromolecules*, 2006, **7**, 1389–1392.
39 S. R. Gondi, A. P. Vogt and B. S. Sumerlin, *Macromolecules*, 2007, **40**, 474–481.
40 D. S. Germack and K. L. Wooley, *J. Polym. Sci., Part A: Polym. Chem.*, 2007, **45**, 4100–4108.
41 C. J. Dürr, L. Hlalele, A. Kaiser, S. Brandau and C. Barner-Kowollik, *Macromolecules*, 2013, **46**, 49–62.
42 R. Nicolay, Y. Kwak and K. Matyjaszewski, *Macromolecules*, 2008, **41**, 4585–4596.
43 D. J. Keddie, *Chem. Soc. Rev.*, 2014, **43**, 496–505.
44 M. D. Rausch, W. P. Hart and D. W. Macomber, *J. Macromol. Sci., Chem.*, 1981, **A16**, 243–250.
45 M. T. Blankenbuehler and J. P. J. Selegue, *Organomet. Chem.*, 2002, **642**, 268–274.
46 A. J. Inglis, T. Pauloehrl and C. Barner-Kowollik, *Macromolecules*, 2010, **43**, 33–36.
47 D. J. am Ende, D. C. Whritenour and J. W. Coe, *Org. ProcessRes. Dev.*, 2007, **11**, 1141–1146.
48 C. Barner-Kowollik, *Macromol. Rapid Commun.*, 2009, **30**, 1625–1631.
49 C. M. Preuss and C. Barner-Kowollik, *Macromol. Theory Simul.*, 2011, **20**, 700–708.

